Effects of O_2 adsorption on secondary electron emission properties

Zhao-Lun Yang(杨兆伦)[1,2], Jing Yang(杨晶)[2], Yun He(何鋆)[2], Tian-Cun Hu(胡天存)[2], Xin-Bo Wang(王新波)[2], Na Zhang(张娜)[2], Ze-Yu Chen(陈泽煜)[2], Guang-Hui Miao(苗光辉)[2], Yu-Ting Zhang(张雨婷)[2], and Wan-Zhao Cui(崔万照)[1,2,†]

[1] *College of Aeronautics, Nanjing University of Aeronautics and Astronautics, Nanjing* 211106, *China*
[2] *National Key Laboratory of Science and Technology on Space Microwave, China Academy of Space Technology (Xi'an), Xi'an* 710100, *China*

(Received 25 July 2022; revised manuscript received 29 August 2022; accepted manuscript online 8 September 2022)

The surface adsorption of gas molecules is a key factor limiting the secondary electron yield (SEY) of a material in many areas of applied physics. The influence of O_2 adsorption on the SEY of metallic Ag is investigated in this work. To account for the particle distribution, we propose a BET theory based on multilayer O_2 physisorption model. Furthermore, based on the phenomenological model of secondary electron (SE) emission and by taking into account the different scattering processes between electrons and particles in the adsorbed layer, we develop a numerical model of SEY in the adsorbed state using Monte Carlo simulations. The relationships among O_2 adsorption, adsorption layer thickness, and SEY variation characteristics are then examined through a series of experiments. After 12-h exposure to O_2, the clean samples increases 12%–19% of the maximum value of SEY and 2.3 nm in thickness of the adsorbed layer. Experimental results are also compared with the results from the MC model to determine whether the model is accurate.

Keywords: multilayer adsorption model, secondary electron, Monte Carlo simulation, gas adsorption experiments

PACS: 79.20.Hx, 79.60.Dp **DOI:** 10.1088/1674-1056/ac904b

1. Introduction

Secondary electron (SE) emission (SEE) refers to the emission of electrons from a solid surface when it is irradiated by a particle with a specific energy. The secondary electron yield (SEY), which is defined as the ratio of the number of emitted electrons to the number of primary electrons (PE), is a crucial parameter describing the capability of SE emission. Current researches focus on the phenomenon of SE emission by using scanning electron microscopy (SEM), Auger electron spectroscopy (AES), and surface microanalysis. Various devices, including electron multiplier tubes, photomultiplier tubes, and microchannel plates, utilize the SEE to detect weak photoelectronic signals.[1] Nevertheless, it is also a major element governing the performances of electron accelerators, high-power microwave sources, and space microwave devices.[2] The electron cloud and multiplicator effect resulting from SE multiplication will significantly degrade performance and even cause irreparable harm.[3,4] With the operating power of spacecraft microwave systems increasing, the degradation of component performance resulting from multipactor is becoming a more serious problem.[5] Clearly, reducing the SEY is an effective method for minimizing electron cloud or multipactor effects.[6] To minimize the electron cloud effects in accelerators or to increase the multiple compressor threshold of microwave components, numerous efforts have been made to reduce the SEY of materials by constructing special surfaces with a variety of microstructures or coatings.[7] The SE typically escapes from the surface at a depth of approximately one free path. Consequently, in addition to the material types and morphology, surface properties such as adsorption, contamination, and oxidation have significant influences on SEY.

This topic has been a focus of numerous studies. The changes in SEY of TiN and DLC samples exposed to oxygen and water vapour were discussed in Ref. [8]. The SEY for gas physisorption on Al and Cu substrates were presented in Ref. [9], where it was discovered that on these substrates, the SEY values from the large area coverage depend solely on the physisorbed species but not on the substrate. By studying the SEY effects of rare gas condensation layers, several hypotheses were proposed in Ref. [10] to explain this effect, including an increase in grain size, charging mechanism effects, and SE reflection effects at the film/solid interface. The changes of work function caused by surface contamination and oxidation were calculated in Ref. [11] by using a theoretical analysis. The effect of atmospheric exposure on the SEY of Au was studied in Ref. [12]. A surface adsorption layer composed of carbon and oxygen elements was discovered to be the source of the increase in SEY. By using the Monte Carlo method, a three-dimensional numerical model was established in Ref. [13] to simulate how electrons and molecules adhere to a surface scatter against each other.

The SEY properties of various contaminants in different substrates have been extensively investigated. At the macroscopic level, some specific experiments have revealed that

[†]Corresponding author. E-mail: cuiwanzhao@126.com

© 2023 Chinese Physical Society and IOP Publishing Ltd

SEY properties can be influenced by factors such as surface topography, ambient pressure, and adsorption types. At the microscopic level, studies have attempted to explain those phenomena from different perspectives, such as changes in surface barrier potential, and reflection at the film/solid interface. However, most of current studies have clarified the properties in the adsorbed state, but the description of the process is still insufficient. Fewer studies have combined adsorption processes with SE emission theory, but the studies of the adsorption volumes are still lacking, therefore, the research on them is very necessary, which not only assists in identifying the factors influencing the SEE characteristics, but also is useful in evaluating the space microwave device applications.

In this work, the effect of gas exposure on the SEY of an inert metal is investigated, and a corresponding SEY simulation model is established; O_2 and metal Ag are selected as our research objects. First, a multilayer adsorption model is created by using the BET theory to determine the distribution of O_2 molecules on the Ag substrate surface. Next, using the Monte Carlo method, a numerical model is developed to investigate the scattering processes of electrons and adsorbed molecules, and SEY properties in the adsorbed state can be obtained through simulations. The effect of O_2 adsorption on SEY and gas desorption are tested in the laboratory to confirm that the relevant theoretical model is accurate.

2. Simulation modules

The simulation consists of a multilayer gas adsorption analysis and an electron collision section, which will be described in the following.

2.1. Multilayer adsorption model

The BET equations are appropriate for describing multilayer physical adsorption surfaces. In this equation, it is assumed that the molecules in the same layer do not interact with one another and that the heat of adsorption in the first layer is a constant based on the interaction between the gas and the surface, whereas the adsorption heat is different in the second and third layers, and other layers based on the interaction forces between each gas molecule.[14]

Assuming that the surface fraction covering only one molecular layer accounts for the total number of molecules on the surface and is denoted by θ_1, the fraction covering two molecular layers is marked as θ_2, the fraction covering i molecular layers and the fraction not covering any molecular layers are, respectively, represented by θ_i and θ. They satisfy the following requirement:

$$\theta_0+\theta_1+\theta_2+\cdots+\theta_i=\theta_0+\sum_{i=1}^{\infty}\theta_i=1. \tag{1}$$

In equilibrium, each θ_i is a constant. σ_0 is the number of molecules per unit area at which the monomolecular layer is completely covered. The total number of molecules adsorbed in the multilayer is

$$\sigma=\sigma_0\theta_1+2\sigma_0\theta_2+\cdots+i\sigma_0\theta_i=\sigma_0\sum_{i=1}^{\infty}i\theta_i. \tag{2}$$

As the equilibrium between adsorption and desorption is achieved, the number of gas molecules in each layer remains constant. A given net increase in θ_i must correspond to its net decrease. For θ_i it is specified that

$$v\theta_{(i-1)}+\left(\frac{\sigma_0}{\tau_{\mathrm{a}(i-1)}}\right)\theta_{(i+1)}=v\theta_i+\left(\frac{\sigma_0}{\tau_{\mathrm{a}i}}\right)\theta_i. \tag{3}$$

For molecular coverings of more than two layers, the condition $\tau_{\mathrm{a}2}=\tau_{\mathrm{a}3}=\cdots=\tau_{\mathrm{a}i}$ can be used to derive the total number in unit area:

$$\sigma_{\mathrm{a}}=\frac{\tau_{\mathrm{a}1}\sigma_0 x}{(1+x)(1-x+\tau_{\mathrm{a}1}x)}, \tag{4}$$

$$x=\frac{p\tau_{\mathrm{a}2}}{\sigma_0(2\pi\mu kT)^{1/2}}=\frac{p}{q}. \tag{5}$$

The symbols p, μ, k, and T denote surface pressure, adsorption relative molecular mass, Boltzmann constant (1.38×10^{-23} J/K), and absolute temperature, respectively. The value $\tau_{\mathrm{a}2}$ represents the enthalpy of evaporation of the adsorbent, and $\tau_{\mathrm{a}1}$ is the heat of adsorption of the adsorbent to the substrate, which can be calculated by determining the residence time of the particles on the surface.

$$\tau_{\mathrm{a}1}=4.58T\cdot\lg\left(7.6\times10^{-4}\frac{V_0\sqrt{\mu T}}{\tau_0 S_0 p}\right). \tag{6}$$

In Eq. (6), V_0 is the adsorption capacity, and S_0 is the specific surface area and can be expressed as $S_0=V_{\mathrm{m}}\cdot N_{\mathrm{A}}\cdot\sigma$, where V_{m}, N_{A}, and σ are saturated adsorption capacity of one molecular layer, Avogadro's constant, and molecular cross-sectional area of adsorbent, respectively. The σ relates to the molecular characteristics of the adsorbent, and density ρ, and is expressed as $\sigma=1.091\,(\mu/N_{\mathrm{A}}\rho)^{2/3}$. In Eq. (6), τ_0 is the period of vibration of the adsorbed molecule, perpendicular to the surface, and it is approximately equal to 10^{-13} s. According to the above analyses, the final equation for multilayer adsorption is

$$\theta=\frac{\sigma_{\mathrm{a}}}{\sigma_0}=\frac{\tau_{\mathrm{a}1}p/q}{(1-p/q)(1-p/q+\tau_{\mathrm{a}1}p/q)}. \tag{7}$$

When p approaches to q, the denominator will be close to 0 and the adsorption coverage approaches to infinity. For physical adsorption, it is observed that as p approaches to the saturation vapour pressure P_0, the amount of adsorption approaches to infinity. So, commonly, q is considered to be equal to P_0. In the adsorption process, the more active molecules are always adsorbed first, and the less active molecules are always adsorbed last. As a result, the heat of adsorption decreases as the amount of adsorption increases across the entire surface

and less active adsorption sites remain unchanged. In addition, the interactions between adsorbed molecules occur as the amount of adsorption increases, which also affects the adsorption process.

Considering the characteristics of gas adsorption on the metal surface, the gas molecule density exhibits an exponentially decreasing distribution, from which the thickness of the adsorbed layer, h, can be deduced as shown below:

$$\int_0^h (C_1 \exp(-C_2 \cdot z) + p/kT)\,\mathrm{d}z \approx \int_0^h C_1 \exp(-C_2 \cdot z)\,\mathrm{d}z = \sigma_\mathrm{a}, \tag{8}$$

where σ_a is the coverage per unit area under a given pressure p, z is the surface normal height, and C_1 and C_2 are both constants.

We use O_2 as an adsorbent and Ag as a substrate in this study. The calculated value of σ at standard atmospheric pressure is 7.4×10^{14}. The coverage is calculated to be about 0.90, indicating that 6.7×10^{14} O_2 molecules have been adsorbed.

2.2. Electron collision model

The electron scattering process could take place in both the adsorbed layer and the Ag substrate. When PEs enter into the adsorbed layer from the outside, they collide with the adsorbed molecules and produce SEs within the layer. Several electrons, including inner SEs and PEs, return to the exterior after multiple collisions to form final SEs. Some electrons enter into the interior of the substrate, while others are depleted in the adsorbed layer as a result of multiple collisions that deplete their energy. The electrons that enter into the substrate continue to scatter with the Ag atoms, where a series of elastic and inelastic collisions will generate SEs. Some SEs pass through the surface barrier and return to the adsorbed layer, where they continue scattering with the adsorbed molecules. Owing to energy loss, others are depleted within the substrate.

Elastic or inelastic backscattered electrons result from collisions between electrons and substrate. Both types of collisions generate a single electron emission. In the initial instance, PEs are perfectly reflected. In the second case, electrons penetrate the substrate, change trajectories, and lose energy in internal scattering multiple times before escaping from the substrate surface. In the case of real secondary emission, the electrons interact with the substrate with a certain probability in a much more complicated way, and a random number of electrons are produced. There have been multiple probability, statistical, and phenomenological models for simulating the scattering of SEs from metal.[15,16] In this subsection, a phenomenological model and Monte Carlo (MC) simulation method are used to simulate the SE emission process.[17] This method has the benefit of producing results that are as close as possible to the actual ones. Fitting the simulations to experimental results on a cleaned surface and using them as a starting point can provide a more accurate analysis of the influence on the SEY adsorption layer.

The simulation of the adsorption layer portion is described in Ref. [13], which describes a three-dimensional numerical model, with which the scattering processes between electrons and adsorbed molecules is simulated. The type of scattering, energy loss, and scattering angle can be determined by the differential scattering cross section for a given incident energy and angle, which is obtained by cubic spline interpolation. Electrons with specific energy will scatter with material atoms or adsorbed molecules; therefore, each electron must be tracked to its final state, either depleted in the adsorbed layer or emitted to the exterior and never returning.

Table 1. Scattering types in model.

S/N	Scattering type	Scattering process	Electron motion state
1	elastic scattering	$e+O_2 \rightarrow O_2+e$	direction change
2	electron excitation	$e+O_2 \rightarrow O_2^{(*)}+e$	energy loss and direction change
3	dissociation	$e+O_2 \rightarrow O^{(*)}+O+e$	
4	ionization	$e+O_2 \rightarrow O_2^+ +2e$ $e+O_2 \rightarrow O+O^+ +2e$	ionization electron generation, energy loss and direction change
5	dissociative attachment	$e+O_2 \rightarrow O+O^-$	

In this model, we account for five types of scatterings between an electron and an O_2 molecule *i.e.*, elastic scattering, electron excitation, dissociation, ionization, and dissociative attachment as shown in Table 1. In MC simulation, elastic scattering between an electron and a neutral molecule only modifies the electron's direction. Because the mass of the O_2 molecule is much greater than that of the electron, the electron energy remains nearly unchanged. The process of excitation and dissociation will result in a loss of electron energy and a modification of the scattering angle. When the energy of the electron exceeds the ionization threshold of an O_2 molecule, new ionization electrons and corresponding ions (O_2^+, O^+) can be produced upon collision of the electron with the adsorbed molecules. The ionization and dissociative attachment processes affect not only the energy and scattering angle of incident electrons, but also their incident number.

The collision procedure can be described roughly as follows. The collision cross-section is used to generate a sequence of intervals, and random numbers are then used to determine the scattering type. The scattering type, energy loss, and scattering angle are then calculated based on the differential scattering cross section obtained by cubic spline interpolation for a given incident energy and angle. Data on the collision cross-section at various energy values can be found in Ref. [18]. For elastic scattering, the scattering angle is anisotropic and can be defined as

$$\mathrm{RND} = \frac{\int_0^{\theta} (\sigma(E_0, \vartheta)\sin\vartheta \,\mathrm{d}\vartheta)\mathrm{d}z}{\int_0^{\pi} (\sigma(E_0, \vartheta)\sin\vartheta \,\mathrm{d}\vartheta)\mathrm{d}z}, \tag{9}$$

where $\sigma(E, \theta)$ is the elastic differential scattering cross section of the corresponding energy E. The data in Ref. [19] provide the angular distribution of electrons elastically scattered from O_2 as a function of energy. The inelastic scattering angle is isotropic and complies to cosine distribution $\cos\theta = 1 - 2(\mathrm{RND})$. The free path length of the electron can be calculated from the $S_n = -\ln(\mathrm{RND})/\rho\sigma_T$, where ρ is the adsorbed molecular density and σ_T is total scattering cross section. If $S_n < h$, the electron collides with the adsorbed molecule. otherwise, the electron is ejected directly as an SE. The path of each electron is simulated by using MC method in order to record all final information about SEs. The main flowchart of the MC simulation is shown in Fig. 1.

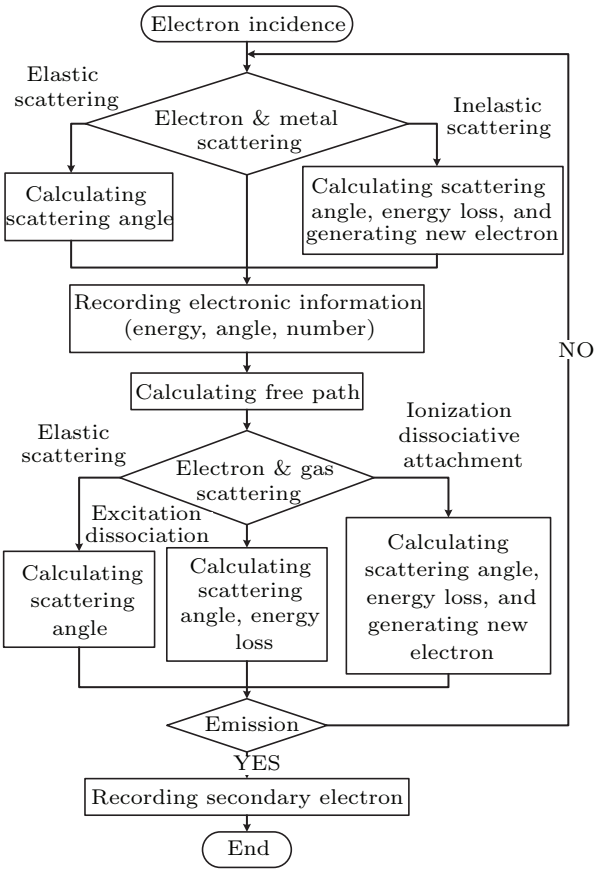


Fig. 1. Flowchart of MC simulation.

Figure 2 illustrates how the SEY varies with the adsorption thickness and primary electron energy. The change of SEY with incident electron energy ranging from 0 eV to 1500 eV is calculated by assuming a starting number of 5×10^4 electrons at each energy point. We cannot exactly determine the value of the adsorption thickness in calculations, so some assumptions need to be made. Using SEY in the clean state as an initial value, and assuming that the number of adsorption densities is in equilibrium, the numbers of SEs of the layers with thickness values of 1 nm, 3 nm, 5 nm, and 10 nm are calculated, respectively. For varying O_2 adsorption thickness, the maximum value of SEY increases, separately, by 5%, 9%, 10%, and 16%.

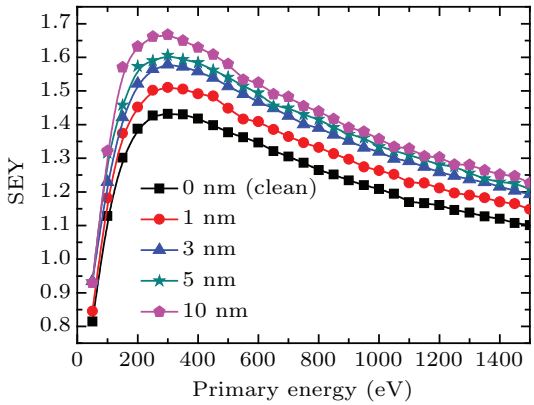


Fig. 2. MC simulation results of SEY at different adsorption thicknesses.

3. Experimental modules

The test stand consists of a vacuum system, an examination system, and a sample-handling system as shown in Fig. 3.[20] The vacuum system includes a load-lock chamber and a main chamber, both of which are sealed by a valve.

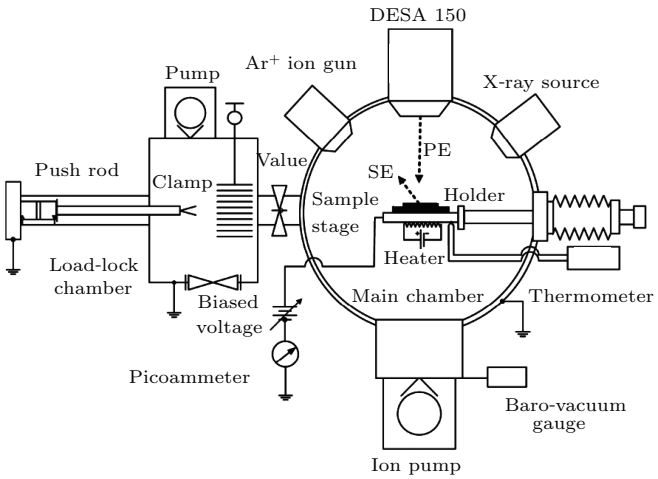


Fig. 3. Schematic diagram of the test stand.

3.1. Desorption experiments

The samples studied were all 0.5-mm thick. These samples were cut into rectangles each with an area of about 1 cm^2 and then they were washed with isopropyl alcohol. Surface

cleaning is the first step, which must be done. A prepared sample was inserted into the main chamber and cleaned for 10 min with Ar-ion at 1 keV under the appropriate conditions.[21] The ion-cleaned sample was then heated with a variable-current resistive heater for 2 h. After completing all of these procedures, the sample surface was relatively clean. The samples were then placed in a load-lock chamber with an oxygen atmosphere at a pressure of 1×10^5 Pa for 12 h for implementing adsorption of oxygen.

The sample was then placed in the main chamber. Owing to the small amount of O_2 adsorbed on the sample, a high vacuum is required for observing subtle changes. The main chamber must be quickly evacuated, as quickly as possible, to a lower pressure state. Next, we closed all valves, forming a main chamber, which became a sealed space. After all preparations were completed, samples were treated by heating and monitoring the change in the pressure of the main chamber.

To ensure that the gas desorption originates primarily from the sample but not the experimental system, two measurements were necessary. In the first measurement, the sample and the holder were heated together, the desorption of the sample and the holder, as well as leakage and gassing of the system would lead to pressure fluctuations. Mo is a low-absorbent metal, which can serve as the holder material. In the second measurement, the same state and operation were maintained as in the first measurement, but only the holder without sample was heated, and the whole pressure change was caused only by the system and the holder. So, the difference in pressure between the two measurements represented the desorption of the sample.

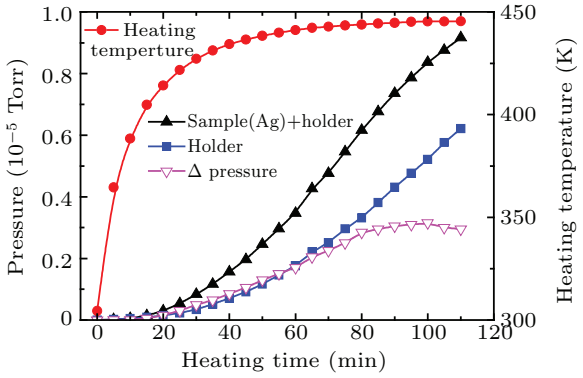


Fig. 4. Measured variations of chamber pressure with temperature and time of heating samples. The unit 1 Torr = 1.33322×10^2 Pa.

As can be seen in Fig. 4, the heating temperature rises from 300 K to 450 K, and as time goes by, the ΔP first increases, then tends to stabilize. The gas equation of state $PV = MRT/\mu$ was used, where V is the volume of the chamber and M is the mass of the desorbed gas, R is a constant that keeps constant regardless of the gas type. We are able to estimate the amount of gas desorbed, which is equivalent to adsorption.

The number of oxygen molecules desorbed was approximately 1.5×10^{15}, which differs by approximately 55% from the above multilayer adsorption model's predictions. The following explains the difference between results. First, the surface of the actual specimen is not flat. The calculation model, however, is based on an ideally flat surface. Moreover, both calculation and experimental procedures are susceptible to error. The data obtained for electron-induced desorption were utilized in the cited source.[22] It has been demonstrated that the number of individual species molecules removed from a Cu surface during processing is less than 10^{16} molecules per square centimeter, which can be used to determine whether the results are plausible.

3.2. XPS analysis

The spectrum was obtained using the DESA 150 electron spectrometer.[23] First, the sample cleaning and O_2 adsorption procedures described previously were repeated. The samples were then loaded into an ultra-high vacuum main vacuum chamber for x-ray photo-electron spectroscopy (XPS) characterization.

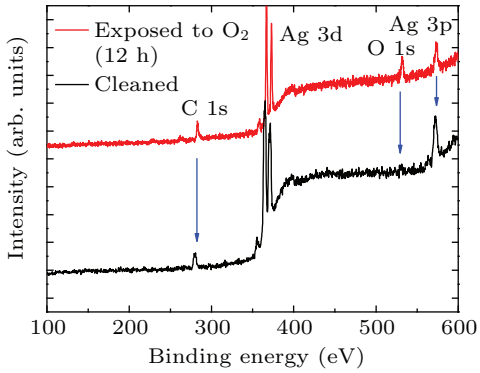


Fig. 5. XPS spectrum of cleaned sample and adsorbed sample.

Figure 5 shows the XPS results for an Ag sample that has been cleaned and adsorbed, respectively. The characteristic peaks of spectra include the photoelectron lines Ag 3d, Ag 3p, C 1s, and O 1s. C 1s and O 1s characteristic peaks, which indicates the presence of carbon and oxygen elements on the surface of Ag. The disappearance of the O 1s peak in the cleaned spectra implies that the adsorbed and contaminated layer on the surface can be eliminated by argon ion sputtering and heating. For the Ag sample exposed to O_2 for 12 h, the quantitative analysis of atomic concentrations reveals an O to Ag ratio of 0.16:1. In addition, the thickness of the adsorption layer can be estimated by using quantitative XPS spectrum analysis and the equation is[24]

$$\frac{I_{O_2}}{I_{Ag}} = \frac{N_{O_2}}{N_{Ag}}\frac{F_{O_2}}{F_{Ag}}\frac{1-\exp(-h/\lambda)}{\exp(-h/\lambda)}, \tag{10}$$

where I is the intensity of the corresponding characteristic peak, N is the atomic density, F is the sensitivity factor, λ

is the inelastic mean free path of the photoelectron, and h is the thickness. The thickness of the adsorption layer for an Ag sample with an exposure time of 12 h was obtained to be 2.32 nm.

3.3. SEY experiments

Figure 3 illustrates the entire experimental setup. The SEY was determined by using the standard sample-current method. Initially, a 500-V bias is applied to the sample, and the sample current is then measured as electrons bombard the metal sample. The majority of SEs excited by electron irradiation have energy values less than 500 eV; therefore, the majority of SEs will return to the metal sample under the action of positive bias, and the sample current at this point is regarded as the incident electron current I_{PE}. To obtain the SE current, a negative bias voltage of -20 V could be applied to the sample, causing the SEs excited by the incident electrons to be repelled by the metal sample. Under action of a negative bias, the sample current was measured to be $I_R = I_{PE} - I_{SE}$, so the SEY is $\delta = 1 - I_R/I_{SE}$. In the main chamber, Ag samples from their initial state were cleaned and adsorbed O_2 then tested. In addition, the calculated results of the SE emission MC model for the O_2 adsorption layer above were presented and compared with the experimental results to verify the model accuracy.

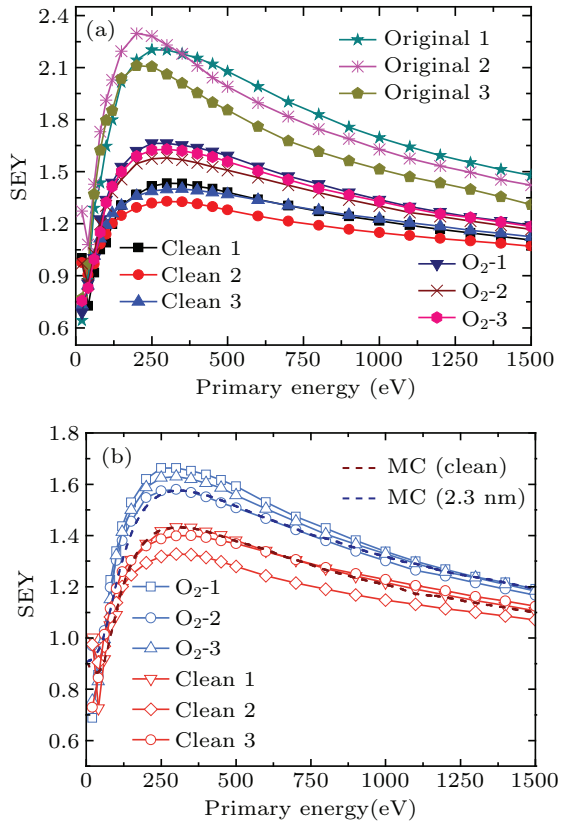


Fig. 6. (a) SEY experimental curves of original, cleaned, and adsorbed samples. (b) Comparison between simulation results and experimental results in clean and adsorbed state comparison.

To reduce testing errors, three samples were evaluated in their original, cleaned, and O_2 adsorbed state, respectively. As depicted in Fig. 6(a), the SEY of the sample in its original state was significantly reduced after the cleaning treatment, indicating that ion bombardment and heating can effectively reduce the SEY of the surface of the sample.[25] The maximum value of SEY for Ag samples in their cleaned state is 1.35–1.43 when PE is between 300 eV and 350 eV. However, the SEY curves in the adsorption state have maximum values varying between 1.56 and 1.63, representing an increase of 14% in SEY. In addition, the test results are compared with the simulations as depicted in Fig. 6(b), where the dashed lines represent the results from the adsorption model for the MC simulation, where the results for the clean state and the adsorption thickness $h = 2.3$ nm are compared, demonstrating the validity of this strategy.

4. Conclusions

The state of adsorption on the material surface and the problem of gas release are taken into account when analyzing the influence of environmental factors on the SE emission characteristics of microwave components during production, transport, and testing, which is also crucial for the study of space microwave components.

In this paper, the effect of O_2 adsorption on the SE emission of Ag is investigated. Initially, a BET theory-based multilayer adsorption model is created to determine the adsorption properties. With a coverage of about 0.90, the calculated number of O_2 adsorbing particles per cm^2 is 6.7×10^{14}. Using the desorption during heating in an experiment, the gas change is determined to be 1.5×10^{15}, which differs by 55% from the results from the multilayer adsorption model. This result can be explained by the fact that the metal surface is not perfectly flat and has slight depressions, resulting in a larger measurement result.

Using the Monte Carlo method, a numerical model is developed to investigate the electron and molecule scattering process. Combining the theory of metal and electron SE emission and the theory of collision between electrons and gas particles yields the variation of SEY in the adsorbed state. With appropriate modifications to the parameters, the model can be used to study the adsorption of different particles on different substrates.

A series of experiments is conducted in which the samples are subjected to ion bombardment and cleaning by heating, followed by exposure to an O_2 atmosphere. The total SEY increases after 12-h exposure, with the lower energy regions changing more greatly, where the increase in SEY maximum value ranges from 12% to 19%. In addition, XPS results indicate the presence of O elements caused by exposure, from which it can be deduced that the thickness of the adsorbed layer is increased by about 2.3 nm. Finally, the validity of the

multilayer adsorption model is determined by comparing pertinent experimental results with the reults from the MC model.

Acknowledgements

Project supported by the Fund from the National Key Laboratory of Science and Technology on Space Mircrowave, China (Grant No. 6142411112205) and the National Natural Science Foundation of China (Grant No. 62001376).

References

[1] Tiras E, Dilsiz K, Ogul H, Southwick D, Bilki B, Wetzel J, Nachtman J, Onel Y and Winn D 2016 *J. Inst.* **11** 10004
[2] Zuo C Y, Gao F and Dai Z L 2018 *Acta Phys. Sin.* **67** 225201 (in Chinese)
[3] Vague J, Melgarejo J C, Guglielmi M, Boria V E, Anza S, Vicente C, Rocio M M, Mariam T, Benito G M and David R 2018 *IEEE Trans. Microw. Theory Tech.* **66** 3644
[4] Wang Z Y, Luo Y, Cui W Z, Wei M, Liang P, J Huangfu, Chen H and Ran L 2009 *Appl. Phys. Lett.* **94** 234101
[5] Mateo-Velez J C, Belhaj M, Dadouch S, Sarrailh P, Hess S L G and Payan D 2019 *IEEE Trans. Plasma Sci.* **47** 3790
[6] Isabel Montero, Leandro Olano, Lydya Aguilera, María E, Dávila, Ulrich Wochner, David Raboso and Petronilo Martín-Iglesias 2020 *J. Electron. Spectrosc. Relat. Phenom.* **241** 146822
[7] Hu J, Cao M, Li Y D, Lin S and Xia N 2018 *Acta Phys. Sin.* **67** 177901 (in Chinese)
[8] Yamamoto K, Shibata T, Ogiwara N and Kinsho M 2007 *Vacuum* **81** 788
[9] Kuzucan A, Herbert Stri and Taborelli M 2012 *J. Vac. Sci. Technol. A* **30** 051401
[10] Cazaux J, Bozhko Y and Hilleret N 2005 *Phys. Rev. B* **71** 035419
[11] Cazaux J 2010 *Appl. Surf. Sci.* **257** 1002
[12] He Y, Shen T, Wang Q, Miao G H, Bai C J, Yu B, Yang J, Feng G B, Hu T C, Wang X B and Cui W Z 2020 *Appl. Surf. Sci.* **520** 146320
[13] Hu X C, Zhang X W, Zhang R and Gu W P 2020 *Results Phys.* **19** 103475
[14] Brunauer S, Emmett P H and Tell E 1938 *J. Am. Chem Soc.* **60** 309
[15] Bai C J, Hu T C, He Y, Miao G H, Wang R, Zhang N and Cui W Z 2021 *Chin. Phys. B* **30** 017901
[16] Cui W Z, Li Y, Zhang H T and Yang J 2022 *Simulation Method of Multipactor and Its Application in Satellite Microwave Components* pp. 23–56 ISBN: 9781003189794
[17] de Lara J, Perez F, Alfonseca M, Galan L, Montero I, Roman E, Baquero Garcia and D R 2006 *IEEE Trans. Plasma Sci.* **34** 476
[18] Yukikazu Itikawa 2009 *J. Phys. Chem.* **38** 1
[19] Jain A 1982 *Phys. Rev. A* **28** 1829
[20] Zhang N, Cao M, Cui W Z and Zhang H B 2014 *Chin. J. Vacuum Sci. Technol.* **34** 554
[21] Hu X C, Zhang H B, Cao M, Zhang N and Cui W Z 2014 *Micron* **64** 52
[22] Baglin V, Collins I, Bernard Henrist, Nol Hilleret and Vorlaufer G 2001 *Large Hadron Collider Projec Report*, 2001, Geneva, August, report 427 Report number: CERN-LHC-Project-Report-472
[23] Li Y, Cui W Z and Wang H G 2015 *Phys. Plasmas* **22** 053108
[24] Nistor V, González L A, Aguilera L, Montero I, Galán L, Wochner U and Raboso D 2014 *Appl. Surf. Sci.* **315** 445
[25] Yang J, Cui W Z, Li Y, Zhang N, Wang R, Hu T C and Zhang H B 2016 *Appl. Surf. Sci.* **382** 88